

# Vector, bidirector, and Bloch skyrmion phases induced by structural crystallographic symmetry breaking

K. C. Erb  and J. Hlinka \**Institute of Physics of the Czech Academy of Sciences, Na Slovance 2, 182 21 Prague 8, Czech Republic*

(Received 9 September 2019; accepted 14 July 2020; published 27 July 2020)

The 212 species of structural phase transitions which break macroscopic symmetry are analyzed with respect to the occurrence of time-reversal-invariant vector and bidirector order parameters. The possibility of discerning the orientational domain states of the low-symmetry phase by these “vectorlike” physical properties has been derived using a computer algorithm exploiting the concept of polar, axial, chiral, and neutral dipoles. It is argued that the presence of a pseudo-Lifshitz invariant of chiral bidirector symmetry in a Ginzburg-Landau functional of uniaxial ferroelectrics can induce electric Bloch skyrmions in the same way as the Dzyaloshinskii-Moriya interaction induces bulk magnetic Bloch skyrmions in chiral magnets. It is found that this is possible for three types of fully ferroelectric phase transitions with a chiral paraelectric phase.

DOI: [10.1103/PhysRevB.102.024110](https://doi.org/10.1103/PhysRevB.102.024110)

## I. INTRODUCTION

Rapidly growing interest in magnetic Bloch skyrmions [1–13] has recently inspired several studies in the field of ferroelectrics [14–21]. Ferroelectric textures with Bloch skyrmion topology have, indeed, been identified in simulations [15–20] and experiments [21]. So far all these ferroelectric textures appear to contain stray-field skyrmions [10,22], i.e., topological defects stabilized by material surfaces and interfaces. Obviously, it is natural to ask whether and when one can also expect bulk ferroelectric Bloch skyrmions, stabilized by a bulk free-energy term, analogous to the chiral Dzyaloshinskii-Moriya term assumed in the canonical magnetic Bloch skyrmion theory [1,23]. In particular, it is worth checking whether the bulk ferroelectric Bloch skyrmion phases are connected to some particular type of symmetry breaking.

## II. MACROSCOPIC SYMMETRY, GENERALIZED DIPOLES, AND SKYRMIONS

When the point group symmetry of a crystal is lowered in response to an isotropic influence like a temperature change, we deal with a macroscopic symmetry-breaking phase transition. It is known that point group symmetry allows one to distinguish 212 distinct species of macroscopic symmetry reduction [24]. Among other things, attribution to a species implies how many new (spontaneous) components of a given tensorial property appear in the low-symmetry phase [24].

Two such properties, spontaneous polarization and spontaneous strain, play a very unique role because they are conjugated to the two most readily available anisotropic thermodynamic forces: the electric field and the stress tensor [25]. However, crystals may develop other properties important in

the context of bulk ferroelectric Bloch skyrmion phases. For example, there are species with a spontaneous axial vector [24] or chiral bidirector [26]. These species describe ferroaxial [27] and chiroaxial [26] phase transitions, respectively. In fact, from the point of view of rotational symmetry, the polar vector  $\mathbf{P}$ , axial vector  $\mathbf{G}$ , chiral bidirector  $\mathbf{C}$ , and neutral bidirector  $\mathbf{N}$  form a complete set of properties that possess only a single axis, a modulus, and a binary sign [28] (see Fig. 1). In that sense, all four vectorlike properties are equally valid for the classification of species and phase transitions.

In the present work, we have found it convenient to extend the analogy even more and generalize the concept of the dipole moment. Obviously, a simple object with polar vector symmetry is an electric dipole, a pair of points with opposite charges. We note that a similarly simple object with the neutral bidirector symmetry  $\mathbf{N}$  is a pair of points with equal charges. Likewise, a pair of points with pseudoscalar properties of opposite signs has the symmetry of the axial vector  $\mathbf{G}$ , and a pair of points with an identical pseudoscalar property has the symmetry of a chiral bidirector  $\mathbf{C}$  (see Fig. 1).

This paper is organized as follows. We first derive general systematic results that are relevant for inspection of the vectorlike symmetry of any crystallographic phase transition. Then we present specific results related to bulk ferroelectric Bloch skyrmions. More specifically, a computer algorithm has been designed to answer, for each vectorlike property  $X$  and for each of the 212 species, the following questions: (i) Is the property  $X$  allowed in the low-symmetry phase, and is there any restriction on the property orientation? (ii) Is the symmetry lowering removing some symmetry restriction on the property  $X$ ? (iii) Does the sign or orientation of the property  $X$  allow one to distinguish all or some orientational domain states? The list of answers yields a table allowing us to find out whether orientational domain states can be fully or partially distinguished by a given vectorlike property. We then extend the argument of Bogdanov and Yablonskii [23] and propose that bulk ferroelectric skyrmion phases can be

\*Corresponding author: [hlinka@fzu.cz](mailto:hlinka@fzu.cz)

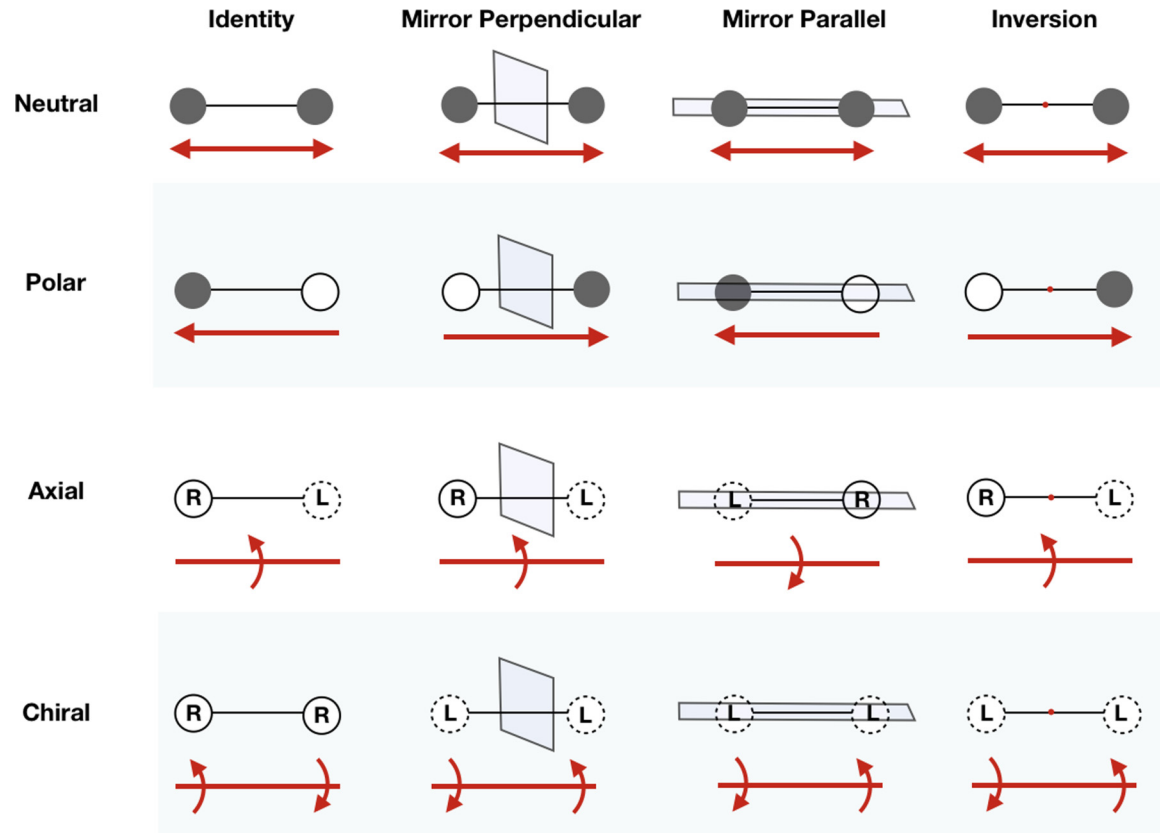


FIG. 1. Transformation properties of four possible time-invariant dipoles. Each row corresponds to one of the dipoles. The first column indicates the name of the dipole property in the row. Each subsequent column indicates the effect of one selected isometry operation on these dipoles, which is either an invariance or a sign reversal. Solid and open circles stand for points with opposite scalar properties, while circles with R and L inside stand for points with opposite pseudoscalar properties (right-handed and left-handed points). Otherwise, the points do not differ in any other internal property.

found in crystals undergoing certain types of nonferroelastic ferroelectric phase transitions. Finally, the derived table is used to identify the desired species.

### III. SYMMETRY-BREAKING SPECIES

Before we present our results, it is worth noting that the concept of species is related to the notion of crystallographic equivalence. A macroscopic crystal symmetry is described by a set of all  $O(3)$  isometries (proper and improper rotations around a fixed point in 3D space) that preserve all macroscopic material properties of the crystal. If there is an isometry in  $O(3)$  that transforms one such crystallographic point group to another one, the two groups are crystallographically equivalent. All symmetry groups linked by such an equivalence relation form a crystallographic class. Any 3D lattice-periodic crystal belongs to one of the 32 crystallographic classes [29,30]. Likewise, a macroscopic symmetry *reduction* is defined by a group-subgroup relation  $G > F$  between point groups  $G$  and  $F$  of the higher- and lower-symmetry crystal phases, respectively. If there is an isometry in  $O(3)$  that transforms the  $G > F$  pair into another pair  $G' > F'$ , the two pairs are equivalent. Symmetry pairs linked by such

equivalence relations constitute one of the 212 macroscopic symmetry-breaking species [24,25].

### IV. METHODOLOGY

The above-introduced question (i) is formally solved by Neumann's principle, which states that a property is allowed if the crystal class is a subgroup of the symmetry of the property [29]. Polar and axial vectors, if allowed, are restricted to a crystallographic axis or within a crystallographic plane or not restricted at all. In contrast, bidirectors, if allowed, could be restricted to an axis or to a triplet of orthogonal axes or to a plane or to a plane and the perpendicular axis or not restricted at all. Figure 2 displays vectorlike property restrictions for groups 222 and 2. In practice, we have designed a computer algorithm that allows one to place a generalized dipole of any of the above types in the center of a crystallographic reference frame and check whether all symmetry operations of a given point group leave such a dipole intact or not. By going through the general and all special positions with respect to the symmetry elements in the group, possible locations of dipoles are found.

Another algorithm was designed to find a group-subgroup representative for each species. The released symmetry con-

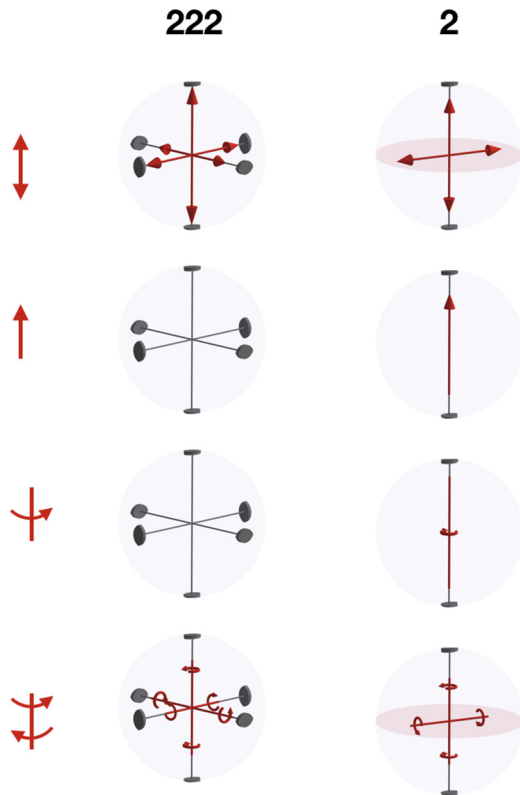


FIG. 2. Symmetry-allowed orientation of vectorlike properties in crystals of 222 and 2 symmetry. Columns correspond to point groups; rows correspond to  $\mathbf{N}$ -,  $\mathbf{P}$ -,  $\mathbf{G}$ -, and  $\mathbf{C}$ -type quantities. The symmetry-unrelated bidirectors have different magnitudes. Under the  $222 > 2$  symmetry lowering, polar and axial vectors appear along the vertical diad, while the bidirectors perpendicular to it are released to have an arbitrary orientation within the indicated plane.

straints on vectorlike properties were obtained by a comparison of the symmetry constraints in the  $G > F$  pair, thus answering question (ii). For example, the species  $222 > 2$  yields new degrees of freedom for all vectorlike properties (see Fig. 2).

Finally, we have investigated whether the property  $X$  allows us to distinguish all or some of the orientational domain states in a given species. Up to three independent generalized dipoles of type  $X$  were placed in the center of a crystallographic reference frame in the most general way compatible with our representative low-symmetry group of a given  $G > F$  species. This gives a unique description of the domain state even in the case of bidirectors. When isometries of the high-symmetry group are applied, either the same or a different dipole configuration is obtained. After going through all symmetry elements of  $G$ , the number of distinct dipole configurations  $n_X$  was counted and compared with the number of orientational domain states  $n$  given by the quotient of the high-symmetry group's order and the lower-symmetry group's order [35].

The numbers of ferroelectric, ferroaxial, and ferrochiral domains match the earlier obtained scores [24,26]. Moreover, we note that the gained neutral bidirector freedom corresponds exactly to the degree of released symmetry constraints on the components of the second-order symmetric polar ten-

sor. Thus, the possibility to distinguish orientational domain states fully or partially by  $\mathbf{N}$  is actually equivalent to full and partial ferroelasticity.

The results are summarized in Fig. 3; full distinction of orientational domain states by the property ( $n_X = n$ ) is marked by the solid circles; partial distinction ( $1 < n_X < n$ ) is marked by the half-filled circles. Species which do not release any additional degree of freedom for the property  $X$  are marked by an open circle. This last situation happens either when  $n_X = 1$  or when the property is not compatible with the symmetry of  $F$  at all ( $n_X = 0$ ). Differentiation between the last two options is quite trivial, so we use a common label there.

## V. FERROELECTRIC DZHALOSHINSKII-MORIYA INTERACTION

Let us now turn back to skyrmions. Originally, the existence of magnetic analogs of Abrikosov vortices, now called skyrmions, was predicted by inspecting solutions of the Ginzburg-Landau potential for a ferromagnet with the free-energy density in the form [23]

$$\frac{1}{2}\alpha(\nabla\mathbf{M})^2 + \frac{1}{2}\beta M_z^2 - M_z H + \gamma w(\mathbf{M}), \quad (1)$$

where  $\alpha$  is the exchange interaction prefactor,  $\beta > 0$  defines the easy-axis anisotropy,  $H$  is the magnetic field along the axis, and  $\gamma$  is the strength of the Dzyaloshinskii-Moriya interaction (DMI) [31–33]. The axisymmetric Bloch skyrmion solution requires that the leading term of the DMI is in the form [23]

$$w = M_z \frac{\partial M_x}{\partial y} - M_x \frac{\partial M_z}{\partial y} - M_z \frac{\partial M_y}{\partial x} + M_y \frac{\partial M_z}{\partial x}. \quad (2)$$

This expression does not depend on the rotation of the coordinates around the  $z$  axis [23]. Actually, a direct check proves that it has the full chiral bidirector symmetry. Therefore, the paramagnetic phase has to allow for a chiral bidirector property along the  $z$  axis. This implies that the Bloch skyrmion model of Eqs. (1) and (2) holds when the paramagnetic phase belongs to class 32, 422, 622, 3, 4, or 6, in agreement with earlier results [23,34].

Let us now assume a ferroelectric material with the same form of free-energy expansion. Consequently, such a hypothetical material should allow for similar axisymmetric Bloch skyrmion soliton solutions. When Eqs. (1) and (2) are written for the electric polarization  $\mathbf{P}$  and electric field  $\mathbf{E}$ , Eq. (1) describes a proper uniaxial ferroelectric crystal close to a second-order nonferroelastic phase transition. Interestingly, the pseudo-Lifshitz term

$$w = P_z \frac{\partial P_x}{\partial y} - P_x \frac{\partial P_z}{\partial y} - P_z \frac{\partial P_y}{\partial x} + P_y \frac{\partial P_z}{\partial x}, \quad (3)$$

analogous to Eq. (2), still transforms as a chiral bidirector. Thus, the postulated form of free-energy expansion of the skyrmion host imposes the same symmetry limitations on phase  $G$  as in the case of the previously considered magnetic skyrmion hosts. Since proper ferroelectricity implies full ferroelectricity [35], by inspection of Fig. 3, it can easily be found that there are only three species that

No.	G	F	n	↑	↓	↗	↘	↖	↙	No.	G	F	n	↑	↓	↗	↘	↖	↙	No.	G	F	n	↑	↓	↗	↘	↖	↙	No.	G	F	n	↑	↓	↗	↘	↖	↙									
1	$\bar{1}$	1	2	○	○	○	○	○	○	54	$4/mmm$	$mmm$	2	●	○	○	○	○	○	107	$6mm$	6	2	○	○	○	○	○	○	160	$m\bar{3}$	1	24	●	○	○	○	○	161	432	23	2	○	○	○	○	○	
2	2	1	2	●	●	●	●	●	●	55	$4/mmm$	$2_1mm$	4	○	○	○	○	○	○	108	$6mm$	$3m$	2	○	○	○	○	○	○	162	432	32	4	○	○	○	○	○	○	163	432	3	8	○	○	○	○	○
3	$m$	1	2	●	●	●	●	●	●	56	$4/mmm$	$2_2mm$	4	○	○	○	○	○	○	109	$6mm$	3	4	○	○	○	○	○	○	164	432	422	3	○	○	○	○	○	○	165	432	4	6	○	○	○	○	○
4	$2/m$	$m$	2	○	○	○	○	○	○	57	$4/mmm$	222	4	○	○	○	○	○	○	110	$6mm$	$2_1mm$	3	●	○	○	○	○	○	166	432	$22_+2$	6	○	○	○	○	○	○	167	432	$22_2$	6	○	○	○	○	○
5	$2/m$	2	2	○	○	○	○	○	○	58	$4/mmm$	$2/m_1$	4	○	○	○	○	○	○	111	$6mm$	$m_-$	6	●	○	○	○	○	168	432	$2_+$	12	○	○	○	○	○	○	169	432	$2_1$	12	○	○	○	○	○	
6	$2/m$	$\bar{1}$	2	○	○	○	○	○	○	59	$4/mmm$	$2/m_-$	4	○	○	○	○	○	○	112	$6mm$	$2_1$	6	○	○	○	○	○	170	432	1	24	○	○	○	○	○	○	171	$\bar{4}3m$	23	2	○	○	○	○	○	
7	$2/m$	1	4	○	○	○	○	○	○	60	$4/mmm$	$m_1$	8	○	○	○	○	○	○	113	$6mm$	1	12	○	○	○	○	○	172	$\bar{4}3m$	$3m$	4	○	○	○	○	○	○	173	$\bar{4}3m$	3	8	○	○	○	○	○	
8	222	2	2	●	●	●	●	●	●	61	$4/mmm$	$m_-$	8	○	○	○	○	○	○	114	$\bar{6}m2$	$\bar{6}$	2	○	○	○	○	○	174	$\bar{4}3m$	$\bar{4}2_+m$	3	○	○	○	○	○	○	175	$\bar{4}3m$	$\bar{4}$	6	○	○	○	○	○	
9	222	1	4	○	○	○	○	○	○	62	$4/mmm$	$2_1$	8	○	○	○	○	○	○	115	$\bar{6}m2$	$3m$	2	○	○	○	○	○	176	$\bar{4}3m$	$2_+m_1m$	6	○	○	○	○	○	○	177	$\bar{4}3m$	$22_+2$	6	○	○	○	○	○	
10	$2mm$	$m$	2	○	○	○	○	○	○	63	$4/mmm$	$2_-$	8	○	○	○	○	○	○	116	$\bar{6}m2$	32	2	○	○	○	○	○	178	$\bar{4}3m$	$m_1$	12	○	○	○	○	○	○	179	$\bar{4}3m$	$2_+$	12	○	○	○	○	○	
11	$2mm$	2	2	○	○	○	○	○	○	64	$4/mmm$	$\bar{1}$	8	○	○	○	○	○	○	117	$\bar{6}m2$	3	4	○	○	○	○	○	180	$\bar{4}3m$	1	24	○	○	○	○	○	○	181	$m\bar{3}m$	$\bar{4}3m$	2	○	○	○	○	○	
12	$2mm$	1	4	○	○	○	○	○	○	65	$4/mmm$	1	16	○	○	○	○	○	○	118	$\bar{6}m2$	$2_2mm$	3	○	○	○	○	○	182	$m\bar{3}m$	432	2	○	○	○	○	○	○	183	$m\bar{3}m$	$m\bar{3}$	2	○	○	○	○	○	
13	$mmm$	$2mm$	2	○	○	○	○	○	○	66	3	1	3	○	○	○	○	○	○	119	$\bar{6}m2$	$m_1$	6	○	○	○	○	○	184	$m\bar{3}m$	23	4	○	○	○	○	○	○	185	$m\bar{3}m$	$\bar{3}m$	4	○	○	○	○	○	
14	$mmm$	222	2	○	○	○	○	○	○	67	$\bar{3}$	3	2	○	○	○	○	○	○	120	$\bar{6}m2$	$m_-$	6	○	○	○	○	○	186	$m\bar{3}m$	$3m$	8	○	○	○	○	○	○	187	$m\bar{3}m$	32	8	○	○	○	○	○	
15	$mmm$	$2/m$	2	○	○	○	○	○	○	68	$\bar{3}$	$\bar{1}$	3	○	○	○	○	○	○	121	$\bar{6}m2$	$2_-$	6	○	○	○	○	○	188	$m\bar{3}m$	$\bar{3}$	8	○	○	○	○	○	○	189	$m\bar{3}m$	3	16	○	○	○	○	○	
16	$mmm$	$m$	4	○	○	○	○	○	○	69	$\bar{3}$	1	6	○	○	○	○	○	○	122	$\bar{6}m2$	1	12	○	○	○	○	○	190	$m\bar{3}m$	$4/mmm$	3	○	○	○	○	○	○	191	$m\bar{3}m$	$\bar{4}2_+m$	6	○	○	○	○	○	
17	$mmm$	2	4	○	○	○	○	○	○	70	32	3	2	○	○	○	○	○	○	123	$6/mmm$	$\bar{6}m2$	2	○	○	○	○	○	192	$m\bar{3}m$	$\bar{4}2_m$	6	○	○	○	○	○	○	193	$m\bar{3}m$	$4mm$	6	○	○	○	○	○	
18	$mmm$	$\bar{1}$	4	○	○	○	○	○	○	71	32	$2_-$	3	○	○	○	○	○	○	124	$6/mmm$	$6mm$	2	○	○	○	○	○	194	$m\bar{3}m$	422	6	○	○	○	○	○	○	195	$m\bar{3}m$	$4/m$	6	○	○	○	○	○	
19	$mmm$	1	8	○	○	○	○	○	○	72	32	1	6	○	○	○	○	○	○	125	$6/mmm$	622	2	○	○	○	○	○	196	$m\bar{3}m$	$\bar{4}$	12	○	○	○	○	○	○	197	$m\bar{3}m$	4	12	○	○	○	○	○	
20	4	$2_1$	2	○	○	○	○	○	○	73	$3m$	3	2	○	○	○	○	○	○	126	$6/mmm$	$6/m$	2	○	○	○	○	○	198	$m\bar{3}m$	$mm_+m$	6	○	○	○	○	○	○	199	$m\bar{3}m$	$mm_1m$	6	○	○	○	○	○	
21	4	1	4	○	○	○	○	○	○	74	$3m$	$m_-$	3	○	○	○	○	○	○	127	$6/mmm$	$\bar{6}$	4	○	○	○	○	○	200	$m\bar{3}m$	$2_+m_+m$	12	○	○	○	○	○	○	201	$m\bar{3}m$	$2_+m_1m$	12	○	○	○	○	○	
22	$\bar{4}$	$2_1$	2	○	○	○	○	○	○	75	$3m$	1	6	○	○	○	○	○	○	128	$6/mmm$	6	4	○	○	○	○	○	202	$m\bar{3}m$	$2_2mm$	12	○	○	○	○	○	○	203	$m\bar{3}m$	$22_+2$	12	○	○	○	○	○	
23	$\bar{4}$	1	4	○	○	○	○	○	○	76	$\bar{3}m$	$3m$	2	○	○	○	○	○	○	129	$6/mmm$	$\bar{3}m$	2	○	○	○	○	○	204	$m\bar{3}m$	$22_2$	12	○	○	○	○	○	○	205	$m\bar{3}m$	$2/m_+$	12	○	○	○	○	○	
24	$4/m$	$\bar{4}$	2	○	○	○	○	○	○	77	$\bar{3}m$	32	2	○	○	○	○	○	○	130	$6/mmm$	$3m$	4	○	○	○	○	○	206	$m\bar{3}m$	$2/m_1$	12	○	○	○	○	○	○	207	$m\bar{3}m$	$m_+$	24	○	○	○	○	○	
25	$4/m$	4	2	○	○	○	○	○	○	78	$\bar{3}m$	$\bar{3}$	2	○	○	○	○	○	○	131	$6/mmm$	32	4	○	○	○	○	○	208	$m\bar{3}m$	$2_+$	24	○	○	○	○	○	○	209	$m\bar{3}m$	$2_1$	24	○	○	○	○	○	
26	$4/m$	$2/m_1$	2	○	○	○	○	○	○	79	$\bar{3}m$	3	4	○	○	○	○	○	○	132	$6/mmm$	$\bar{3}$	4	○	○	○	○	○	210	$m\bar{3}m$	$2_1$	24	○	○	○	○	○	○	211	$m\bar{3}m$	$\bar{1}$	24	○	○	○	○	○	
27	$4/m$	$m_1$	4	○	○	○	○	○	○	80	$\bar{3}m$	$2/m_-$	3	○	○	○	○	○	○	133	$6/mmm$	3	8	○	○	○	○	○	212	$m\bar{3}m$	1	48	○	○	○	○	○	○										
28	$4/m$	$2_1$	4	○	○	○	○	○	○	81	$\bar{3}m$	$m_-$	6	○	○	○	○	○	○	134	$6/mmm$	$mmm$	3	○	○	○	○	○																				
29	$4/m$	$\bar{1}$	4	○	○	○	○	○	○	82	$\bar{3}m$	$2_-$	6	○	○	○	○	○	○	135	$6/mmm$	$2_1mm$	6	○	○	○	○	○																				
30	$4/m$	1	8	○	○	○	○	○	○	83	$\bar{3}m$	$\bar{1}$	6	○	○	○	○	○	○	136	$6/mmm$	$2_2mm$	6	○	○	○	○	○																				
31	422	4	2	○	○	○	○	○	○	84	$\bar{3}m$	1	12	○	○	○	○	○	○	137	$6/mmm$	222	6	○	○	○	○	○																				
32	422	222	2	○	○	○	○	○	○	85	6	3	2	○	○	○	○	○	○	138	$6/mmm$	$2/m_1$	6	○	○	○	○	○																				
33	422	$2_1$	4	○	○	○	○	○	○	86	6	$2_1$	3	○	○	○	○	○	○	139	$6/mmm$	$2/m_-$	6	○	○	○	○	○																				
34	422	$2_-$	4	○	○	○	○	○	○	87	6	1	6	○	○	○	○	○	○	140	$6/mmm$	$m_1$	12	○	○	○	○	○																				
35	422	1	8	○	○	○	○	○	○	88	$\bar{6}$	3	2	○	○	○	○	○	○	141	$6/mmm$	$m_-$	12	○	○	○	○	○																				
36	$4mm$	4	2	○	○	○	○	○	○	89	$\bar{6}$	$m_1$	3	○	○	○	○	○	○	142	$6/mmm$	$2_1$	12	○	○	○	○	○																				
37	$4mm$	$2_1mm$	2	○	○	○	○	○	○	90	$\bar{6}$	1	6	○																																		

binations. The idea of generalized dipoles can be extended to multipoles and time-odd properties [39–45], and the point group symmetry-breaking analysis also applies to many other areas of physics. In addition, it was realized that the ferroelectric analog of a chiral DMI has the symmetry of a chiral dipole. This observation was used to predict a scenario for the appearance of bulk ferroelectric Bloch skyrmion phases

in materials with  $32 > 3$ ,  $422 > 4$ , or  $622 > 6$  symmetry breaking.

#### ACKNOWLEDGMENT

This work was supported by the Czech Science Foundation (Project No. 19-28594X).

- [1] U. K. Rößler, A. N. Bogdanov, and C. Pfleiderer, Spontaneous skyrmion ground states in magnetic metals, *Nature (London)* **442**, 797 (2006).
- [2] S. Mühlbauer, B. Binz, F. Jonietz, C. Pfleiderer, A. Rosch, A. Neubauer, R. Georgii, and P. Böni, Skyrmion lattice in a chiral magnet, *Science* **323**, 915 (2009).
- [3] A. Neubauer, C. Pfleiderer, B. Binz, A. Rosch, R. Ritz, P. G. Niklowitz, and P. Böni, Topological Hall Effect in the Phase of MnSi, *Phys. Rev. Lett.* **102**, 186602 (2009).
- [4] C. Pappas, E. Lelièvre-Berna, P. Falus, P. M. Bentley, E. Moskvina, S. Grigoriev, P. Fouquet, and B. Farago, Chiral Paramagnetic Skyrmion-like Phase in MnSi, *Phys. Rev. Lett.* **102**, 197202 (2009).
- [5] X. Z. Yu, Y. Onose, N. Kanazawa, J. H. Park, J. H. Han, Y. Matsui, N. Nagaosa, and Y. Tokura, Real-space observation of a two-dimensional skyrmion crystal, *Nature (London)* **465**, 901 (2010).
- [6] A. Fert, V. Cros, and J. Sampaio, Skyrmions on the track, *Nat. Nanotechnol.* **8**, 152 (2013).
- [7] F. N. Rybakov, A. B. Borisov, and A. N. Bogdanov, Three-dimensional skyrmion states in thin films of cubic helimagnets, *Phys. Rev. B* **87**, 094424 (2013).
- [8] N. Romming, C. Hanneken, M. Menzel, J. E. Bickel, B. Wolter, K. von Bergmann, A. Kubetzka, and R. Wiesendanger, Writing and Deleting Single Magnetic Skyrmions, *Science* **341**, 636 (2015).
- [9] N. Romming, A. Kubetzka, C. Hanneken, K. von Bergmann, and R. Wiesendanger, Field-Dependent Size and Shape of Single Magnetic Skyrmions, *Phys. Rev. Lett.* **114**, 177203 (2015).
- [10] F. Büttner, I. Lemesch, and G. Beach, Theory of isolated magnetic skyrmions: From fundamentals to room temperature applications, *Sci. Rep.* **8**, 4464 (2018).
- [11] F. N. Rybakov and N. S. Kiselev, Chiral magnetic skyrmions with arbitrary topological charge, *Phys. Rev. B* **99**, 064437 (2019).
- [12] S. M. Dahir, A. F. Volkov, and I. M. Eremin, Interaction of Skyrmions and Pearl Vortices in Superconductor-Chiral Ferromagnet Heterostructures, *Phys. Rev. Lett.* **122**, 097001 (2019).
- [13] N. Mathur, M. J. Stolt, and S. Jin, Magnetic skyrmions in nanostructures of non-centrosymmetric materials, *APL Mater.* **7**, 120703 (2019).
- [14] J. M. Gregg, Exotic Domain States in Ferroelectrics: Searching for Vortices and Skyrmions, *Ferroelectrics* **433**, 74 (2012).
- [15] Y. Nahas, S. Prokhorenko, L. Louis, Z. Gui, I. Kornev, and L. Bellaïche, Discovery of stable skyrmionic state in ferroelectric nanocomposites, *Nat. Commun.* **6**, 8542 (2015).
- [16] Z. Hong and L.-Q. Chen, Blowing polar skyrmion bubbles in oxide superlattices, *Acta Mater.* **152**, 155 (2018).
- [17] M. A. P. Gonçalves, C. Escorihuela-Sayalero, P. García-Fernández, J. Junquera, and J. Íñiguez, Theoretical guidelines to create and tune electric skyrmion bubbles, *Sci. Adv.* **5**, eaau7023 (2019).
- [18] I. Luk'yanchuk, Y. Tikhonov, A. Razumnaya, and V. M. Vinokur, Hopfions emerge in ferroelectrics, *Nat. Commun.* **11**, 2433 (2020).
- [19] J. Hlinka and P. Ondrejko, Skyrmions in ferroelectric materials, *Solid State Phys.* **70**, 143 (2019).
- [20] S. Prosandeev, S. Prokhorenko, Y. Nahas, and L. Bellaïche, Prediction of a novel topological multidefect ground state, *Phys. Rev. B* **100**, 140104(R) (2019).
- [21] S. Das, Y. L. Tang, Z. Hong, M. A. P. Gonçalves, M. R. McCarter, C. Klewe, K. X. Nguyen, F. Gómez-Ortiz, P. Shafer, E. Arenholz, V. A. Stoica, S.-L. Hsu, B. Wang, C. Ophus, J. F. Liu, C. T. Nelson, S. Saremi, B. Prasad, A. B. Mei, D. G. Schlom, J. Íñiguez, P. García-Fernández, D. A. Muller, L. Q. Chen, J. Junquera, L. W. Martin, and R. Ramesh, Observation of room-temperature polar skyrmions, *Nature (London)* **568**, 368 (2019).
- [22] N. S. Kiselev, A. N. Bogdanov, R. Schäfer, and U. K. Rößler, Comment on “Giant Skyrmions Stabilized by Dipole-Dipole Interactions in Thin Ferromagnetic Films,” *Phys. Rev. Lett.* **107**, 179701 (2011).
- [23] A. N. Bogdanov and D. A. Yablonskii, Thermodynamically stable “vortices” in magnetically ordered crystals. The mixed state of magnets, *Zh. Eksp. Teor. Fiz.* **95**, 178 (1989).
- [24] J. Hlinka, J. Privratska, P. Ondrejko, and V. Janovec, Symmetry Guide to Ferroaxial Transitions, *Phys. Rev. Lett.* **116**, 177602 (2016).
- [25] K. Aizu, Possible species of ferromagnetic, ferroelectric, and ferroelastic crystals, *Phys. Rev. B* **2**, 754 (1970).
- [26] K. C. Erb and J. Hlinka, Symmetry Guide to Chiroaxial Transitions, *Phase Transitions* **91**, 953 (2018).
- [27] R. D. Johnson, L. C. Chapon, D. D. Khalyavin, P. Manuel, P. G. Radaelli, and C. Martin, Giant Improper Ferroelectricity in the Ferroaxial Magnet CaMn<sub>7</sub>O<sub>12</sub>, *Phys. Rev. Lett.* **108**, 067201 (2012).
- [28] J. Hlinka, Eight Types of Symmetrically Distinct Vectorlike Physical Quantities, *Phys. Rev. Lett.* **113**, 165502 (2014).
- [29] R. Newnham, *Properties of Materials: Anisotropy, Symmetry, Structure* (Oxford University Press, Oxford, 2005).
- [30] V. Janovec, Axial crystals - macroscopic symmetry and tensor properties, *Phase Transit.* **90**, 1 (2017).
- [31] I. E. Dzyaloshinskii, Thermodynamical Theory of “Weak” Ferromagnetism in Antiferromagnetic Substances, *Sov. Phys. JETP* **5**, 1259 (1957).
- [32] I. E. Dzyaloshinskii, A thermodynamic theory of “weak” ferromagnetism of antiferromagnetics, *J. Phys. Chem. Sol.* **4**, 241 (1958).
- [33] T. Moriya, Anisotropic Superexchange Interaction and Weak Ferromagnetism, *Phys. Rev.* **120**, 91 (1960).

- [34] I. E. Dzyaloshinskii, Theory of helicoidal structures in antiferromagnets. I. Nonmetals, *Sov. Phys. JETP* **19**, 960 (1964).
- [35] V. Janovec, V. Dvorak, and J. Petzelt, Symmetry classification and properties of equitranslation structural phase transitions, *Czech J. Phys. B* **25**, 1362 (1975).
- [36] P.-F. Li, W.-Q. Liao, Y.-Y. Tang, W. Qiao, D. Zhao, Y. Ai, Y.-F. Yao, and R.-G. Xiong, Organic enantiomeric high- $T_c$  ferroelectrics, *Proc. Natl. Acad. Sci. USA* **116**, 5878 (2019).
- [37] B. T. Mathias and J. P. Remeika, Ferroelectricity of Dicalcium Strontium Propionate, *Phys. Rev.* **107**, 1727 (1957).
- [38] Strictly speaking, the Bogdanov-Yablonskii scenario of Eqs. (1) and (2) might not be the only possibility for the formation of bulk ferroelectric Bloch skyrmion textures since polarization might appear as a secondary order parameter.
- [39] Y. Tanaka, T. Takeuchi, S. W. Lovesey, K. S. Knight, A. Chainani, Y. Takata, M. Oura, Y. Senba, H. Ohashi, and S. Shin, Right Handed or Left Handed? Forbidden X-Ray Diffraction Reveals Chirality, *Phys. Rev. Lett.* **100**, 145502 (2008).
- [40] S. W. Lovesey, A. Rodríguez-Fernández, and J. A. Blanco, Parity-odd multipoles, magnetic charges, and chirality in hematite  $\alpha$ -Fe<sub>2</sub>O<sub>3</sub>, *Phys. Rev. B* **83**, 054427 (2011).
- [41] S.-W. Cheong, D. Talbayev, V. Kiryukhin, and A. Saxena, Broken symmetries, non-reciprocity, and multiferroicity, *npj Quantum Mater.* **3**, 19 (2018).
- [42] S. Hayami, M. Yatsushiro, Y. Yanagi, and H. Kusunose, Classification of atomic-scale multipoles under crystallographic point groups and application to linear response tensors, *Phys. Rev. B* **98**, 165110 (2018).
- [43] P. Lazzeretti, Chiral discrimination in nuclear magnetic resonance spectroscopy, *J. Phys.: Condens. Matter* **29**, 443001 (2017).
- [44] P. Lazzeretti, Current density tensors, *J. Chem. Phys.* **148**, 134109 (2018).
- [45] P. Lazzeretti, Frequency-dependent current density tensors as density functions of dynamic polarizabilities, *J. Chem. Phys.* **150**, 184117 (2019).